KIMIKA Volume 33, Number 2, pp. 44-58 (2022)
 ISSN 2508-0911
https://doi.org/10.26534/kimika.v32i2.44-58

Synthesis of Gold Nanoparticles (AuNPs) Using Salt-Soluble Wheat Flour Proteins and Their Use in the Fluorescence-based Sensing of Folic Acid

Carlos Antonio N. Concepcion, Maritess M. Lacquio, Milagros M. Peralta and Mariam C. Recuenco*

Institute of Chemistry, University of the Philippines Los Baños, Brgy. Batong Malake, Los Baños, Laguna 4031

*Author to whom correspondence should be addressed; email: mcrecuenco@up.edu.ph

ABSTRACT

Protein-stabilized metal nanoparticles have been receiving significant attention because their optical properties could be used for sensing applications. This study describes the synthesis of gold nanoparticles (AuNPs) stabilized with salt-soluble proteins extracted from wheat flour, and their use in the fluorescence-based detection and quantification of folic acid. The salt-soluble protein extract from defatted wheat flour contained at least eight components with molecular weights ranging from 7.26 to 57.0 kDa. The extract was made alkaline and then mixed with a $HAuCl_4$ solution to synthesize the AuNPs. The wheat-AuNPs were red in color and had a surface plasmon resonance (SPR) peak at 519 nm. Based on the UV-visible spectrum, the AuNPs may have ~3.4 nm average size. The AuNPs exhibited fluorescence emission at 734 nm upon excitation at 365 nm. The fluorescence quenching of the AuNPs observed upon incremental addition of folic acid (0 to 10 μg mL^{-1}) was fitted to the Stern-Volmer equation. From the Stern-Volmer plot, the limits of linearity (LOL), detection (LOD), and quantitation (LOQ) were determined as 22.0 μg mL^{-1}, 0.92 μg mL^{-1}, and 3.1 μg mL^{-1}, respectively. Several substances, including some metal ions, were tested for their effects on the AuNPs' fluorescence. Moreover, a proposed fluorescence-based folic acid quantification was evaluated by determining the folic acid content of several pharmaceutical formulations.

Keywords: *folic acid, gold nanoparticles, wheat proteins, fluorescence quenching, Stern-Volmer equation*

INTRODUCTION

Folic acid (FA, (2*S*)-2-[(4-{[(2-amino-4-hydroxypteridin-6-yl)methyl]amino}phenyl)formamido] -pentanedioic acid), also known as vitamin B9 or folacin, is a water-soluble compound with roles in metabolic pathways and involved in cell development and maintenance (Blom et al., 2011). Deficiencies in FA can lead to higher risks of heart disease and congenital defects (Blom et al.,

2011). Because of its importance, FA-containing products, such as food supplements and enriched or fortified foods had been manufactured to prevent deficiencies (Di Tinno et al., 2021). Demands for FA quantification methods, especially in pharmaceutical formulations (Zhao et al., 2006), are on the rise to assess how certain formulations or supplements should be used. This is crucial since the risks of excessive ingestion of FA could mask possible deficiencies of another important B-vitamin, vitamin B12 or cobalamin (Ribeiro et al., 2016). The standard method of determination is a microbiological assay (MA) involving the turbidimetric bacterial growth of *Lactobacillus casei* that is proportional to the amount of FA (Rahman et al., 2015). Though MA has high reliability and accuracy, the method can be susceptible to other growth factors and can be time-consuming. High-performance liquid chromatography (HPLC) offers a useful alternative for FA analysis (Jastrebova et al., 2003). However, HPLC-based methods could have high operating costs, sizable consumption of samples and solvents, and can generate difficult-to-dispose organic wastes. There were also proposed electroanalytical methods (Flores et al., 2005) and spectrophotometric techniques (Nagaraja et al., 2002; Anastasopoulos et al., 2007). Still, some of these methods can be laborious and have low sensitivity.

Metal nanoparticles have been receiving attention because of their interesting size-dependent optical properties appropriate for a range of applications. Metal nanoparticles are composed of clusters of metal atoms with sizes of 1.0 nm to 100 nm (Ghosh and Pal, 2007). The particles exhibit a characteristic absorption in the visible region due to surface plasmon resonance (SPR), which is the oscillation of electrons between the conduction and valence bands of the metal caused by the interaction of electrons with the electric fields of light (Kelly et al., 2013). On the other hand, because of their discontinuous band structures and quantum confinement, metal nanoparticles can fluoresce in the visible region of the electromagnetic spectrum when excited with near-ultraviolet radiation (Zheng et al., 2012). Gold is commonly used in preparation due to its stability and non-reactivity relative to other metals such as silver and copper (Zheng et al., 2007). AuNPs tend to aggregate into larger clusters, hence capping agents are used to ensure long-term stability (Housni et al., 2008). Proteins had been demonstrated to be capable of reducing metal ions and stabilizing metal nanoparticle preparations (Xie et al., 2009). Protein-stabilized AuNPs are biocompatible and are frequently utilized in biomedical applications such as drug delivery (Rastogi et al., 2012), diagnostic imaging (Zu et al., 2016), and cancer therapy (Chiu et al., 2018). They are also employed as sensors for the determination of various chemical species, from metal ions (Lee and Huang, 2011) and small compounds (Huang et al., 2012) to large macromolecules (Cui et al., 2008).

Wheat proteins are important in relation to the baking quality of wheat, mainly attributed to their viscoelastic properties (Veraverbeke and Delcour, 2002). Wheat proteins constitute two distinct protein fractions: non-gluten and gluten proteins. Non-gluten fractions include albumins and globulins, which consist of enzymes, enzyme inhibitors, structural proteins, and storage proteins. Gluten fractions include gliadins and glutenins, which are largely responsible for dough visco-elasticity and are divided based on solubilities in alcoholic solutions. These four major protein types are typically separated sequentially using a series of appropriate solvents (Lookhart and Bean, 1995). Generally, wheat proteins can be acquired by using inexpensive and readily accessible reagents such as 2-propanol, sodium chloride, and water (DuPont et al., 2005). Most of the wheat proteins also have considerable stability to heat and in weak acids and bases, which contributes to ease in preparation and storage. With the availability and relatively low costs of wheat flour, the usage of wheat proteins in applied biochemistry may help reduce costs in general research.

This study aimed to provide a simple, inexpensive, and environment-friendly approach to the synthesis of AuNPs stabilized with salt-soluble wheat proteins, and their use in the detection and quantification of folic acid through fluorescence quenching. Preliminary observations on the responses of these fluorescent protein stabilized AuNPs to folic acid and several other chemical species revealed the potential in the development of a method for folic acid determination.

METHODOLOGY

Materials and Equipment. The wheat flour sample used was the *SM Bonus All-Purpose Flour* brand. Gold (III) chloride trihydrate and folic acid were purchased from Sigma-Aldrich. Sample pharmaceutical formulations used for FA determination were *Folicap*®, *Biogesic*®, and *Centrum*® *Advance*. Absorption measurements for the Bradford assay were obtained using the Milton Roy Co. Spectronic 21D UV-Visible Spectrophotometer. The UV-Visible absorption spectrum of wheat-AuNPs was obtained using the Thermo Scientific™ Multiskan™ FC Microplate Photometer. Fluorescence emission spectra and measurements for wheat-AuNPs were obtained using the Shimadzu RF-5301PC Fluorescence Spectrophotometer.

Extraction of Salt-Soluble Wheat Proteins. Extraction of albumin and globulins was adapted from Sandiford et al. (1997), with modifications. Wheat flour was defatted with n-hexane for about 1 h. Albumins and globulins were extracted by stirring 10 g defatted wheat flour in 50 mL 0.5 M NaCl for 1 h at room temperature. Supernatants containing the wheat proteins were obtained by centrifugation (10000 g, 25 °C, 15 min) of the flour-salt mixture.

Quantification of Salt-Soluble Wheat Proteins. The Bradford assay (1976) was employed for protein quantification. Protein standards used were 0 to 2.0 mg mL^{-1} BSA solutions. The assay was performed by mixing 20 µL protein extract or standard with 1.0 mL Bradford reagent, incubating the solutions for 5 min, and measuring their absorbances at 595 nm. The concentration of the protein extract was determined by interpolation from an absorbance (A) vs. concentration ([$protein$]) calibration curve constructed using the BSA standards, in reference to the Beer-Lambert law, shown below. Molar absorptivity (a) and path length (b) were kept constant.

$$A = ab[protein]$$

Characterization of Salt-Soluble Wheat Proteins. Laemmli's (1970) SDS-PAGE protocol was performed for the electrophoresis of wheat proteins. A 15% polyacrylamide resolving gel was cast in the electrophoresis setup followed by a 4% polyacrylamide stacking gel, and a running buffer was poured into the setup. Protein extracts (25 µL) were mixed with a sample buffer (25 µL). The mixtures were shaken vigorously, heated to 95 °C, and loaded to the wells of the stacking gel, along with protein markers. The electrophoretic run was done at room temperature and 100 V. Coomassie Blue gel staining was performed to visualize the protein bands. Molecular weights (MWs) of the protein samples were estimated by interpolation from a retention factor (*Rf*) vs. *log MW* calibration curve constructed using the protein markers.

$$Rf = \frac{distance\ traveled\ by\ the\ band}{distance\ traveled\ by\ the\ dye\ front}$$

Synthesis of Wheat-AuNPs. The synthesis of AuNPs stabilized by salt-soluble wheat proteins, designated as wheat-AuNPs, was adapted from the synthesis of BSA-stabilized gold nanoclusters of Xie et al. (2009), with modifications. The wheat protein extract (10 mL, 1.132 mg mL^{-1}) was first stirred with 3 M NaOH (226 µL) at room temperature for 5 min. The resulting solution was then stirred vigorously with 200 mM $HAuCl_4$ (113 µL) at room temperature for 30 min. The final mixture was allowed to stand overnight in a dark place at room temperature. Figure 1 shows the scheme for the extraction of salt-soluble proteins from wheat followed by wheat-AuNP synthesis.

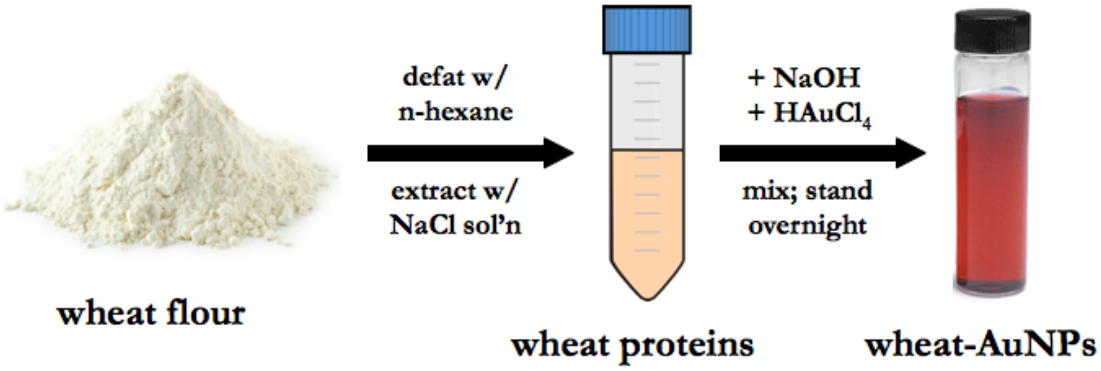

Figure 1. Simplified schematic diagram for the extraction of salt-soluble proteins from wheat flour and the synthesis of wheat-AuNPs.

Characterization of Wheat-AuNPs. The UV-visible absorption spectrum of the wheat-AuNPs mixture was acquired from 400 nm to 800 nm. The fluorescence emission spectrum of a solution of wheat-AuNPs, diluted to 20 volumes with distilled water, was acquired from 500 to 900 nm with 305 nm to 395 nm excitation wavelengths at 15 nm intervals and 15-nm excitation and emission slit widths.

Fluorescence Quenching of Wheat-AuNPs by Folic Acid. The wheat-AuNPs were diluted to 20 volumes with distilled water prior to analysis. Standard FA solution (1000 μg mL^{-1}) was added to the diluted wheat-AuNPs (2.0 mL) at 4.0-μL increments. The fluorescence spectrum from 685 to 785 nm was acquired for each FA addition (0 to 20 μL), with 365 nm as the excitation wavelength. The procedure was repeated three times on different days. Another identical experiment was performed with the FA addition increased up to 100 μL. For each experiment, the initial (I_0) to final (I) ratio of fluorescence intensities at 734 nm (365 nm excitation) were plotted against the FA concentrations ($[FA]$), in reference to the Stern-Volmer equation, shown below. Slopes or Stern-Volmer constants (K_{SV}) were determined by simple linear regression.

$$\frac{I_0}{I} = 1 + K_{SV}[FA]$$

The limits of detection (LOD) and quantitation (LOQ) of the fluorescence quenching experiment were calculated from the standard deviation of the lowest concentration signal (s) and slope of the calibration curve (m), shown below.

$$LOD = \frac{3s}{m} \qquad\qquad LOQ = \frac{10s}{m}$$

Effect of Other Chemical Species on Wheat-AuNP Fluorescence. Diluted (20x) wheat-AuNPs (2.0 mL) were mixed with 1000-μg mL^{-1} solutions of various biological compounds and metal ions (40 μL each). The biological compounds used were glucose, sucrose, starch, glycine, histidine, cysteine, ascorbic acid, acetic acid, gallic acid, urea, citrate, and lactate. Metal ions used were Na^{+}, K^{+}, Ca^{2+}, Al^{3+}, Ni^{2+}, Cu^{2+}, Co^{2+}, Fe^{3+}, and Ti^{4+}. Fluorescence intensities of the diluted wheat-AuNPs at 734 nm (365 nm excitation) were recorded before and after the addition of each chemical species.

Folic Acid Determination in Pharmaceutical Formulations using Wheat-AuNPs. Three formulations were used for the experiment: *Folicap*® (pure FA), *Biogesic*® (no FA), and *Centrum*® *Advance* (FA + other chemical species). *Folicap*® capsules (3 pieces) were emptied of their contents and 15 mL 0.1 M NaOH was added to the powder. *Biogesic*® and *Centrum*®

Advance tablets (3 pieces each) were homogenized and 12 mL 0.1 M NaOH was added to each powder. The suspensions were mixed for 5 min at room temperature and the extracts were obtained through centrifugation (10000 g, 25 °C, 5 min.). Samples (20 µL) for analysis were added to a dilute solution of wheat-AuNPs (100 µL wheat-AuNPs and 1.88 mL distilled water). Fluorescence intensities of the wheat-AuNPs at 734 nm (365 nm excitation) were measured before and after the addition of the samples. The FA contents of the formulations were determined by the method of external calibration using a standard calibration curve produced using FA standards, with the Stern-Volmer equation as the working equation. Analysis for recovery was performed on the *Folicap*® samples by spiking them with standard FA (1000 µg mL^{-1}) at increasing concentrations (0 to 6.0 µg mL^{-1}), performing the same fluorescence analysis, and computing the percentage of found FA concentration relative to expected FA concentration.

RESULTS AND DISCUSSION

Extraction of Salt-Soluble Wheat Proteins. The salt extraction of defatted wheat flour produced a clear pale-yellow solution having a final volume of approximately 42 mL. Wheat flour consists of four distinct components: starches, lipids, non-starch polysaccharides, and wheat proteins (Goesaert et al., 2005). Starches are insoluble in aqueous media due to their polymeric structures. Lipids are also insoluble due to their hydrophobic nature. Non-starch polysaccharides include arabinoxylans, β-glucan, cellulose, and arabinogalactan-peptides, where some of which are soluble in aqueous media (Goesaert et al., 2005). The salt-soluble extract obtained may contain the non-gluten proteins, albumins and globulins, and some non-starch polysaccharides.

The protein concentration of the extract was 1.131 mg mL^{-1} while the total protein extracted was 47.51 mg, which was 0.4751% by mass of defatted wheat flour. The reported composition of wheat flour included 10 to 12% protein, where 15 to 20% of these proteins are albumins and globulins (Goesaert et al., 2005). Based on this report, non-gluten proteins should constitute about 1.5 to 2.4% of the flour mass. The amount of total protein extracted was about three to five times lower than the amounts of non-gluten proteins reported. To increase the efficiency of extraction, it may be necessary to use smaller portions of the 0.5 M NaCl solvent multiple times (Sandiford et al., 1997).

Characterization of Salt-Soluble Wheat Proteins. The salt-soluble wheat protein extract was found to contain at least eight components based on the SDS-PAGE result shown in Figure 2. Molecular weights of the components ranged from 7.26 kDa to 57.0 kDa. The SDS-PAGE profile also provided a good estimation of relative protein amounts, which are proportional to the band intensity. Among the bands seen in Figure 2, the 57.0-kDa band displayed the greatest intensity, followed by the components having MWs of 7.26 kDa and 10.7 kDa. These results suggest that these three components had the highest concentrations in the extract.

Using the estimated MWs, probable identities of the extracted wheat proteins were proposed and presented in Table 1. The UniProt (uniprot.org) database was searched for wheat proteins that were closest to the estimated MWs. The probable identities may include amylase inhibitors, lipid transfer proteins, gliadin precursors, and other enzymes. The SDS-PAGE profile was found to be similar to the profile in Sandiford et al. (1997) where they suggested that the salt-soluble extract contained albumins and globulins. Singh et al. (2001) reported that the water-soluble proteins from Chinese spring flour included amylase inhibitors, gliadin precursors, lipid transfer proteins, globulins, and albumins, determined through N-terminal sequencing. Mass spectrometry could provide more accurate identities of the proteins in the salt-soluble extract. Altenbach et al. (2020) reported that the KCl-soluble fraction of US wheat Butte 86 flour contained some gluten proteins and about 57 different types of non-gluten proteins.

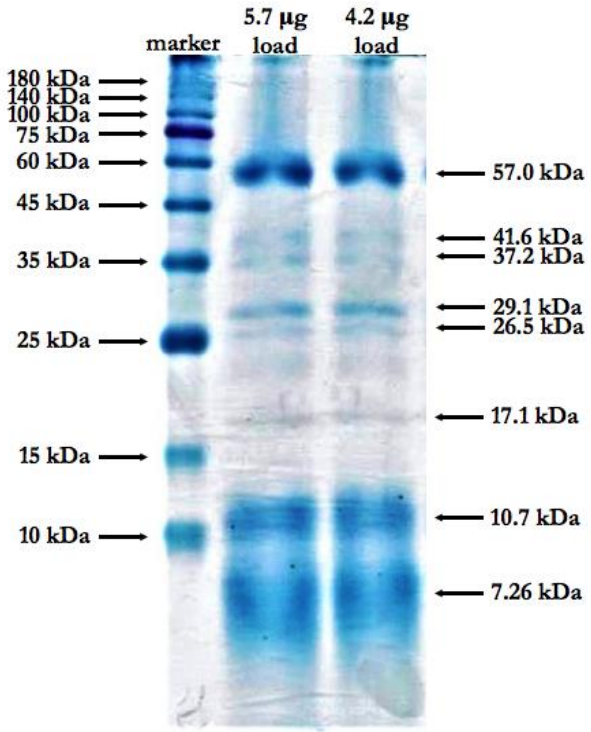

Figure 2. SDS-PAGE profile of the salt-soluble protein extract from wheat flour. The protein extract contained at least eight components with MWs between 7.26 kDa to 57.0 kDa. Electrophoresis run was performed using a 15% polyacrylamide gel SDS-PAGE gel under 100 V potential.

Table 1. Molecular Weights and Some Probable Identities of the Extracted Wheat Proteins.

Band	Experimental MW[a], kDa	Theoretical MW[b], kDa	Probable Identity (Swiss-Prot Accession Number)	% Error[c]
1	7.26	7.05	*non-specific lipid transfer protein* (P82901)	3.09
2	10.68	9.83	*non-specific lipid transfer protein* (P82900)	8.66
3	17.08	16.80	*alpha-amylase inhibitor* (P01083)	1.66
4	26.50	25.83	*glutathione S-transferase* (P30110)	2.61
5	29.14	29.05	*gamma-gliadin precursor* (P08079)	0.31
6	37.18	37.12	*gamma-gliadin precursor* (P08453)	0.15
7	41.62	42.03	*sedoheptulose-1,7 bisphosphatase* (P46285)	-0.99
8	57.01	56.73	*NAD(P)H-quinone oxidoreductase subunit* (P0CD54, P0CD55)	0.49

[a] Values were calculated based on relative mobilities compared to the protein MW markers.
[b] Values were based on the complete sequence of the mature protein.
[c] [|Theoretical MW – Experimental MW|/Theoretical MW] * 100%

Synthesis of Wheat-AuNPs. The AuNP synthesis initially produced a pale-yellow solution, which turned into a red colloidal mixture (Figure 3a, inset), after overnight incubation. The study of Xie et al. (2009) on the green synthesis of protein-stabilized gold nanoclusters included a gold to

protein ratio of 1 mM gold to 5 mg protein. With a 1.131 mg mL^{-1} calculated protein concentration, 113 µL 200 mM $HAuCl_4$ were used, along with 226 µL 3 M NaOH, per 10 mL protein solution for wheat-AuNP synthesis. The characteristic red color of the resulting mixture indicated the existence of AuNPs and hinted at the successful conjugation between the AuNPs and the salt-soluble wheat proteins. The observed color agreed with AuNPs synthesized using citrate (Bastús et al., 2011) and using proteins or peptides (Aldeek et al., 2013; Matei et al., 2019).

The formation of protein-stabilized AuNPs follows a general mechanism, by which wheat-AuNPs could be hypothesized to also follow. The first step is the dispersion of the wheat proteins and gold ions in one mixture allowing the formation of protein-$AuCl_4^-$ complexes (Tan et al., 2010). Upon pH adjustment by NaOH addition, Au^{3+} ions are reduced to Au^+ and Au^0 species by tyrosine residues, developing Au^0 clusters via nucleation (Xie et al., 2009). After a short incubation, there would be the creation of Au^+-S bonds between the cysteine residues of the wheat proteins and gold ions (Xie et al., 2009; Bolaños, 2019). Amino acids such as tryptophan may also participate in the reduction of the gold ions, while cysteine, histidine and methionine may play roles in complex formation (Tan et al., 2010). Following long incubation, further aggregation of the gold clusters, prompted by the need to shoulder lower energy configurations, finally materializes the nanoparticles (Tan et al., 2010).

Characterization of Wheat-AuNPs. Characterization of wheat-AuNPs was accomplished by UV-Visible and fluorescence spectrophotometry.

UV-Visible Spectrophotometry. The UV-Vis absorption spectrum of the wheat-AuNPs is displayed in Figure 3a. The UV-Vis spectrum shows a peak around 519 nm. The presence of this SPR peak in the absorption spectrum, in addition to the red color of the wheat-AuNP mixture, confirmed the existence of AuNPs and their successful production. SPR is the oscillation of electrons between conduction and valence bands of metal when electric fields of light rays interact with them (Amendola et al., 2017). For AuNPs, an absorption at around 515 nm to 570 nm in their UV-Vis spectra gives AuNPs a distinct red color (Haiss et al., 2007).

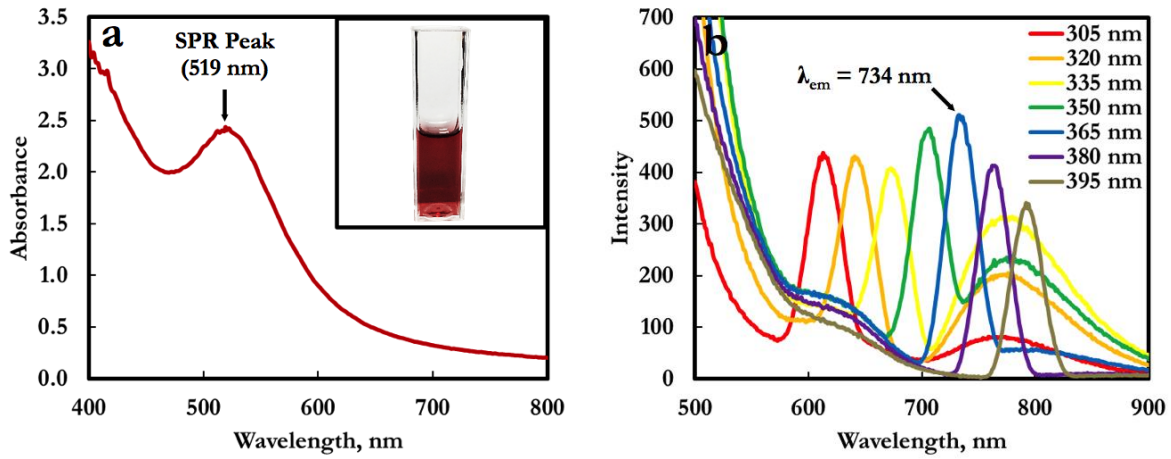

Figure 3. Characterization of the optical properties of the wheat-AuNPs. (a) UV-Visible absorption spectrum of wheat-AuNPs (inset). SPR peak observed at 519 nm, (b) Fluorescence emission spectra of wheat-AuNPs (20x diluted) at 305 to 395 nm excitation. Maximum emission was observed at 734 nm (365 nm excitation).

Information about the shapes (Amendola et al., 2017) and sizes (Haiss et al., 2007) of gold nanoparticles can be determined from their UV-visible spectra. The single SPR peak at 519 nm suggested that the wheat-AuNPs should conform to a spherical geometry, which is consistent with several studies (Housni et al., 2008; Garcia-Hernandez et al., 2019). Based on the proposed model of Haiss et al. (2007) that described the relationship between particle size and SPR absorbances,

the estimated sizes of the wheat-AuNPs should be around 3.4 nm. To establish the shapes and sizes, analysis by scanning or transmission electron microscopy (SEM, TEM) must be performed. From the spectroscopic data, it is plausible that the as-prepared AuNPs consisted of particles with a variety of sizes.

Fluorescence Spectrophotometry. The fluorescence emission spectra of the wheat-AuNPs (20x diluted) are shown in Figure 3b. The emission spectra showed a series of peaks from 613 nm to 792 nm upon excitation with radiation from 305 nm to 395 nm. Maximum intensity (λ_{em}) was seen at 734 nm upon 365 nm excitation. The spectra demonstrated the photoluminescence of the wheat-AuNPs within the visible region. Multiple peaks can be seen on several emission spectra in Figure 3b. Apart from the sharp peak at 734 nm, which can be ascribed to the fluorescence of wheat-AuNPs, there are other signals around 600 and 800 nm. These signals may be attributed to the wheat proteins left in the colloidal mixture from wheat-AuNP synthesis (Mathew and Joseph, 2017), whose fluorescence was said to be caused by their aromatic residues. The fluorescence of protein stabilized AuNPs could be due to much smaller particles or nanoclusters with sizes ˜0.8 nm (Xie et al., 2009). Larger particles (>20 nm) were reported to not exhibit fluorescence (Xie et al., 2009).

Fluorescence of wheat-AuNPs can be associated with electronic transitions that occur between the lowest unoccupied molecular orbitals (LUMOs) in the *sp* band and the highest occupied molecular orbitals (HOMOs) in the *d* band (Zhou et al., 2010). Thiol groups of the wheat protein cysteine residues are π-acceptor ligands, and their *p* orbitals have higher energy than the *d* orbitals of Au^{+} ions (Zhou et al., 2010). Overlap of these orbitals can lead to the formation of metal-to-ligand charge transfer excited states. As a result, excitation can occur between the hybrid MOs, followed by non-radiative vibrational relaxations toward the LUMO of the *sp* band (Zheng et al., 2012). After which, emission can take place between there and HOMOs of the *d* band (Zheng et al., 2012).

Fluorescence Quenching of Wheat-AuNPs by Folic Acid. Standard FA was added in incremental amounts to a 20x diluted wheat-AuNP solution to determine the effects on the fluorescence of wheat-AuNPs. In Figure 4a, the fluorescence intensity of wheat-AuNPs at 365 nm excitation decreases as the concentration of FA increases, indicating the quenching effect of FA on the fluorescence of wheat-AuNPs.

A plausible mechanism for the fluorescence quenching of wheat-AuNPs by FA may be based on FA-tryptophan interactions. From Table 1, the extract could contain proteins that, except for non-specific lipid transfer proteins, have at least two tryptophan residues. FA molecules can bind to the tryptophan residues of the wheat proteins via charge-transfer complex formation (Liang and Subirade, 2010), hydrogen bonding, and hydrophobic forces (Shi et al., 2017). The resulting wheat-AuNP-FA complex becomes non-fluorescent owing to a non-radiative energy transfer from wheat-AuNPs to FA (Mote et al., 2011).

The fluorescence experiment was replicated on different days to determine the reproducibility of the quenching phenomenon. Initial (I_0) to final (I) fluorescence ratios of wheat-AuNPs at 734 nm (365 nm excitation) were plotted against concentrations of FA in the mixture ([FA]), in reference to the Stern-Volmer equation. The plots constructed in Figure 4b presented a consistent linear relationship between the wheat-AuNP fluorescence ratios and FA concentrations.

Stern-Volmer constants (K_{SV}) or slopes of the best fit lines and coefficients of determination (R^2) were obtained from simple linear regression (Table 2). The Stern-Volmer constants ranged from 0.0920 to 0.1001 mL μg^{-1} with an RSD of 3.72% and the coefficients of determination ranged from 0.9659 to 0.9906 with an RSD of 1.15%. The data indicated the repeatability of the linear relationship between the wheat-AuNP fluorescence ratios and FA concentrations (Fajgelj and

Ambrus, 2000). Hence, the proposed method for FA determination was subjected to further validation and figures of merit were calculated.

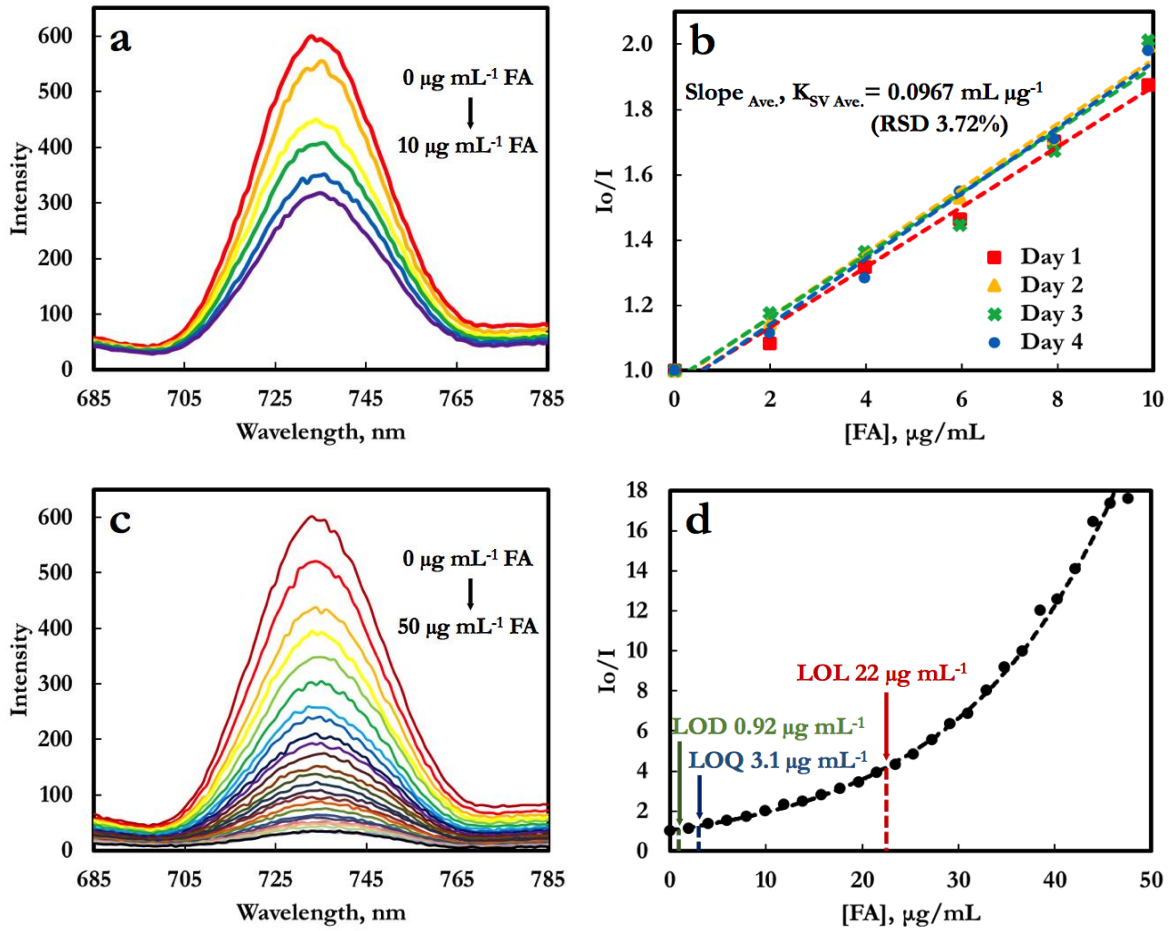

Figure 4. Fluorescence-based sensing of folic acid. (a) Fluorescence quenching of wheat-AuNPs upon addition of FA (0 to 10 µg mL^{-1}). (b) Initial to final wheat-AuNP fluorescence ratios vs. FA concentrations (0 to 10 µg mL^{-1}) at different days. The average Stern-Volmer constant, $K_{SV\ Ave}$ is 0.967 mL µg^{-1} . (c) Extensive fluorescence quenching of wheat-AuNPs upon increased addition of FA (0 to 50 µg mL^{-1}). (d) Initial to final wheat-AuNP fluorescence ratios vs. FA concentrations (0 to 50 µg mL^{-1}). *LOL*, *LOD*, and *LOQ* at 22, 0.92, and 3.1 µg mL^{-1}, respectively.

Table 2. Simple Linear Regression and RSD Analysis of Wheat-AuNP Fluorescence Ratios vs. Folic Acid Concentrations (0 to 10 µg mL^{-1}) at Different Time Periods and Figures of Merit of the Fluorescence Quenching of Wheat-AuNPs by Folic Acid.

Parameter	Time					%RSD [b]
	Day 1	Day 2	Day 3	Day 4	Average	
K_{SV} [a] (mL µg^{-1})	0.0920	0.0988	0.0958	0.1001	0.0967	3.72
R^2	0.9881	0.9906	0.9659	0.9853	0.9825	1.15

Limit of Linearity	*Limit of Detection*	*Limit of Quantitation*
22 µg mL^{-1}	0.92 µg mL^{-1}	3.1 µg mL^{-1}

[a] Stern-Volmer constant
[b] [Standard deviation of K_{SV} values/Mean of K_{SV} values] * 100%

The limit of linearity (LOL) was determined from the data after FA addition was increased up to 50 μg mL^{-1}. The LOL is the FA concentration where the resulting best fit line gives $r \geq 0.99$ (Green, 1996). In the quenching experiment, a continuous decrease in the fluorescence ratio of wheat-AuNPs was observed, even when FA concentration was increased up to 50 μg mL^{-1} (Figures 4c and 4d). An acceptable linear relationship was observed to be lost starting at around 22 μg mL^{-1} (Figure 4d), which indicated the LOL. From the four-day experiment, values of LOD and LOQ were calculated to be 0.92 μg mL^{-1} and 3.1 μg mL^{-1}, respectively. All estimated limits are presented in Table 2. Earlier studies using fluorescence-based analysis using nanoparticles had lower LODs. Hemmateenejad et al. (2014) reported an LOD of 18.3 ng mL^{-1} folic acid using BSA-stabilized gold nanoclusters. Moreover, in the study of Fereja et al, 2021, the use of BSA-capped Au–Ag bimetallic nanoclusters for folic acid analysis had an LOD of 0.47 nM (0.21 ng mL^{-1}). Compared to the previous studies, the as-prepared wheat-AuNPs are highly likely to contain a variety of sizes, unlike the highly uniform nanoparticles or nanoclusters synthesized using highly purified proteins as capping agents.

Effect of Other Chemical Species on Wheat-AuNP Fluorescence. Twelve biological compounds and nine metal ions were subjected to the same fluorescence quenching experiment to test their effects on the fluorescence of wheat-AuNPs. Initial (I_0) to final (I) fluorescence ratios of wheat-AuNPs for each ion or compound in comparison to FA were plotted (Figures 5) to show their relative magnitudes of fluorescence change. Quenching is observed when I is less than I_0 ($I_0/I >$ 1) while an enhancing effect is observed when I is greater than I_0 ($I_0/I <$ 1).

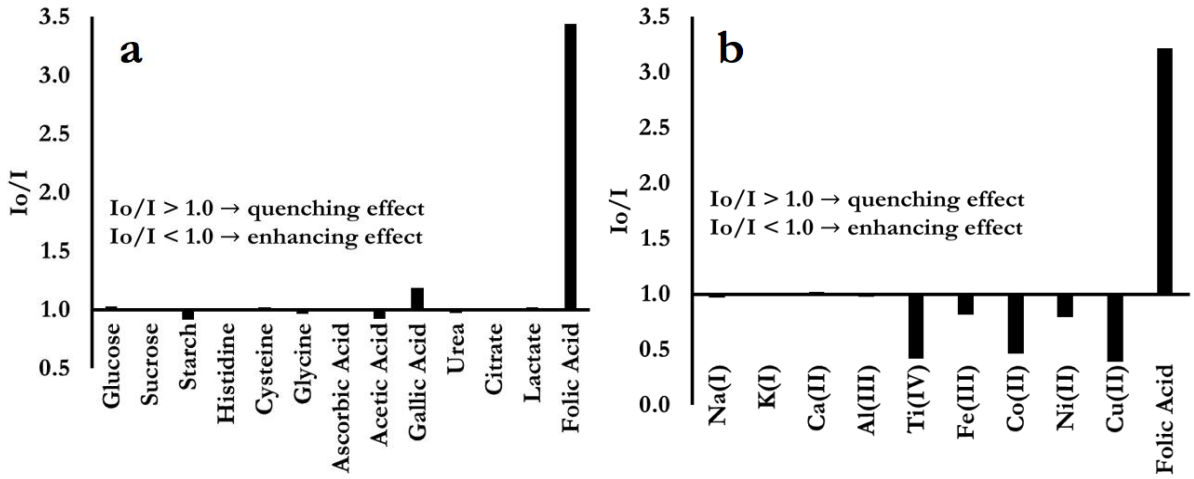

Figure 5. Effect of compounds on the fluorescence of wheat-AuNPs. (a) Biological compounds such as gallic acid, acetic acid, and starch marginally affect wheat-AuNP fluorescence. (b) Metal ions such as Fe^{3+}, Ni^{2+}, Co^{2+}, Ti^{4+}, and Cu^{2+} significantly enhance wheat-AuNP fluorescence.

From Figure 5a, the wheat-AuNPs showed little to no fluorescence changes upon the addition of the biological compounds. Among the substances, starch, gallic acid, and acetic acid had some noticeable effects on the wheat-AuNP fluorescence. From Figure 5b, the wheat-AuNPs displayed substantial fluorescence increases upon the addition of some metal ions. Cu^{2+}, Ti^{4+}, Co^{2+}, Ni^{2+}, and Fe^{3+}, had enhancing effects on wheat-AuNP fluorescence. These metal ions may interfere with FA determination if they are present in the samples for analysis. Results indicate that the fluorescence of wheat-AuNPs can be altered not only by FA but also by other chemical species. Possible interfering substances should be considered in FA determination via fluorescence quenching of wheat-AuNPs. The addition of ethylenediaminetetraacetic acid (EDTA), a heavy metal antagonist, to sequester metal ions could work as a part of sample preparation before the FA determination (Hemmateenejad et al., 2014). Isolation of FA from samples using organic solvent extraction and thin layer chromatography should also be considered in sample preparations.

Folic Acid Determination in Pharmaceutical Formulations using Wheat-AuNPs. The method for FA determination through wheat-AuNP fluorescence quenching was used in the analysis of various pharmaceutical formulations. This aimed to evaluate the applicability of the proposed method to actual samples. For the experiment, three drugs of different constituents (*Folicap*®, *Biogesic*®, and *Centrum*® *Advance*) were used.

The FA content of each formulation was estimated via interpolation from a calibration curve prepared using standard solutions of the analyte (Table 3). Calculations returned 4205 μg of FA per *Folicap*® capsule compared to the 5000 μg of FA declared, with a 15.89% absolute error and 5.55% RSD. For *Centrum*® *Advance* and *Biogesic*®, the fluorescence of wheat-AuNPs was observed to increase after each sample was added, indicating enhancing effects. FA amounts from the data could not be obtained since fluorescence enhancement was not the expected response for the wheat-AuNP and FA interactions. The abundance of components in *Centrum*® *Advance* affected the FA determination. The presence of several transition metal salts (notably cupric sulfate, $CuSO_4$) likely caused a significant increase in wheat-AuNP fluorescence. Acetaminophen in *Biogesic*® may have fluorescence enhancing effects due to the compound also acting as a stabilizing agent for the gold nanoclusters (Rajendran et al., 2019).

Table 3. Folic Acid (FA) Determination in Different Pharmaceutical Formulations Through Fluorescence Quenching of Wheat-AuNPs.

Drug	Calculated FA per tablet/capsule [a], μg	Declared FA per tablet/capsule, μg	%Error [b]	%RSD [c]
Folicap®	4205	5000	15.89	5.55
Biogesic®	n.d.*	0	––	––
Centrum® *Advance*	n.d.*	400	––	––

*n.d. – not determined (negative concentrations calculated)
[a] Values are means of three replicates.
[b] [|Declared FA - Calculated FA|/Declared FA] *100%
[c] [Standard deviation of Calculated FA values/Mean of Calculated FA values] * 100%

In Table 4, recoveries in *Folicap*® samples were 84.10% to 106.1% with 1.89% to 5.55% RSD upon addition of 0 to 5.96 μg mL^{-1} FA. The % recoveries fall within acceptable values (Fajgelj and Ambrus, 2000). However, the FA recoveries were observed to increase when concentrations of the spike were increased. This suggested matrix effects of the drug extract slightly interfering with the detection of FA (Mathew and Joseph, 2017). The matrix effects can be deemed as a possible source of error in the FA determination in the *Folicap*® samples. Additional washing procedures of the solid residue during FA extraction can help better recover FA from the pharmaceutical preparations and improve its determination (Hemmateenejad et al., 2014). The matrix effects could also be addressed by improving the sample preparation protocols.

Table 4. Recoveries of *Folicap*® Upon Addition of Increasing Amounts of Folic Acid (FA) Standard.

Added $[FA]$, μg mL^{-1}	Found $[FA]$ [a], μg mL^{-1}	Expected $[FA]$, μg mL^{-1}	%Recovery [b]	%RSD [c]
0	8.41	10.00	84.10	5.55
2.00	11.28	12.00	94.06	1.89
3.98	14.31	13.98	102.4	3.45
5.96	16.94	15.96	106.1	2.33

[a] Values are means of three replicates.
[b] [Found FA /Expected FA] *100%
[c] [Standard deviation of Found FA values/Mean of Found FA values] * 100%

CONCLUSIONS

This study demonstrated the synthesis of AuNPs using salt-soluble proteins from wheat flour. The as-prepared AuNPs exhibited the distinct and established optical properties of AuNPs such as presence of the SPR absorption, and the fluorescence properties. Utilizing the fluorescence properties of the wheat-AuNPs, a method for the determination of folic acid based on fluorescence quenching was proposed. The proposed method had decent limits of linearity, detection, and quantitation but may encounter some measurement errors in the presence of potentially interfering species such as heavy metal ions. Therefore, it is highly recommended to conduct more work to establish the optimum conditions for a protocol using the wheat-AuNPs for FA determination.

ACKNOWLEDGMENTS

This work was supported by the UPLB Basic Research Program (Project ID 17855).

REFERENCES

Aldeek F, Safi M, Zhan N, Palui G, Mattoussi H. Understanding the self-assembly of proteins onto gold nanoparticles and quantum dots driven by metal-histidine coordination. ACS Nano. 2013 Oct; 7(11):10197–10210. https://doi.org/10.1021/nn404479h

Altenbach SB, Chang HC, Simon-Buss A. Deciphering the immunogenic potential of wheat flour: a reference map of the salt-soluble proteome from the U.S. wheat Butte 86. Proteome Sci. 2020 Aug; 18(8). https://doi.org/10.1186/s12953-020-00164-6

Amendola V, Pilot R, Frasconi M, Maragò OM, Iatì MA. Surface plasmon resonance in gold nanoparticles: A review. J Phys Condens Matter. 2017 Apr; 29(20):203002. https://doi.org/10.1088/1361-648X/aa60f3

Anastasopoulos P, Mellos T, Spinou M, Tsiaka T, Timotheou-Potamia M. Chemiluminometric and fluorimetric determination of folic acid. Anal Lett. 2007 Nov; 40(11):2203–2216. https://doi.org/10.1080/00032710701567022

Bastús NG, Comenge J, Puntes V. Kinetically controlled seeded growth synthesis of citrate-stabilized gold nanoparticles of up to 200 nm: size focusing versus Ostwald ripening. Langmuir. 2011 July; 27(17):11098-11105. https://doi.org/10.1021/la201938u

Blom HJ, Smulders Y. Overview of homocysteine and folate metabolism. With special references to cardiovascular disease and neural tube defects. J Inherit Metab Dis. 2011 Feb; 34(1):75-81. https://doi.org/10.1007/s10545-010-9177-4

Bolaños K, Kogan MJ, Araya E. Capping gold nanoparticles with albumin to improve their biomedical properties. Int J Nanomedicine. 2019 Aug; 14:6387–6406. https://doi.org/10.2147%2FIJN.S210992

Bradford MM. A rapid and sensitive method for the quantitation of microgram quantities of protein utilizing the principle of protein-dye binding. Anal Biochem. 1976 May; 72:248–254. https://doi.org/10.1016/0003-2697(76)90527-3

Chiu HT, Chen CH, Li ML, Su CK, Sun YC, Chiang CS, Huang YF. Bioprosthesis of core-shell gold nanorod/serum albumin nanoimitation: A half-native and half-artificial nanohybrid for cancer

theranostics. Chem Mater. 2018 Dec; 30(3):729–747. https://doi.org/10.1021/acs.chemmater.7b04127

Cui R, Huang H, Yin Z, Gao D, Zhu JJ. Horseradish peroxidase-functionalized gold nanoparticle label for amplified immunoanalysis based on gold nanoparticles/carbon nanotubes hybrids modified biosensor. Biosens Bioelectron. 2008 June; 23(11):1666–1673. https://doi.org/10.1016/j.bios.2008.01.034

Di Tinno A, Cancelliere R, Micheli L. Determination of folic acid using biosensors—a short review of recent progress. Sensors. 2021 May; 21(10):3360. https://doi.org/10.3390/s21103360

DuPont FM, Chan R, Lopez R, Vensel WH. Sequential extraction and quantitative recovery of gliadins, glutenins, and other proteins from small samples of wheat flour. J Agric Food Chem. 2005 Feb; 53(5):1575–1584. https://doi.org/10.1021/jf048697l

Fajgelj A, Ambrus A. Guidelines for single-laboratory validation of analytical methods for trace-level concentrations of organic chemicals. In: Fajgelj A, Ambrus A, editors. Principles and practices of method validation. Londo: Royal Society of Chemistry; 2000. p. 179-252. https://doi.org/10.1039/9781847551757-00179

Fereja SL, Li P, Guo J, Fang Z, Zhang Z, Zhuang Z, Zhang X, Liu K, Chen W. Silver-enhanced fluorescence of bimetallic Au/Ag nanoclusters as ultrasensitive sensing probe for the detection of folic acid. Talanta. 2021 Oct; 233:122469. https://doi.org/10.1016/j.talanta.2021.122469

Flores J, Peñalvo GC, Mansilla AE, Gómez MJR. Capillary electrophoretic determination of methotrexate, leucovorin and folic acid in human urine. J Chromatogr B Anal Technol Biomed Life Sci. 2005 May; 819(1):141–147. https://doi.org/10.1016/j.jchromb.2005.01.039

Garcia-Hernandez C, Freese AK, Rodriguez-Mendez ML, Wanekaya AK. In situ synthesis, stabilization and activity of protein-modified gold nanoparticles for biological applications. Biomater Sci. 2019 Apr; 7(6):2511–2519. https://doi.org/10.1039/C9BM00129H

Ghosh SK, Pal T. Interparticle coupling effect on the surface plasmon resonance of gold nanoparticles: From theory to applications. Chem Rev. 2007 Nov; 107(11):4797–4862. https://doi.org/10.1021/cr0680282

Goesaert H, Brijs K, Veraverbeke WS, Courtin CM, Gebruers K, Delcour JA. Wheat flour constituents: How they impact bread quality, and how to impact their functionality. Trends Food Sci Technol. 2005 Jan-Mar; 16(1–3):12–30. https://doi.org/10.1016/j.tifs.2004.02.011

Green JM. Peer reviewed: a practical guide to analytical method validation. Anal Chem. 1996 May; 68(9):305A-309A. https://doi.org/10.1021/ac961912f

Haiss W, Thanh NTK, Aveyard J, Fernig DG. Determination of size and concentration of gold nanoparticles from UV–vis spectra. Anal Chem. 2007 Apr; 79(11):4215–4221. https://doi.org/10.1021/ac0702084

Hemmateenejad B, Shakerizadeh-Shirazi F, Samari F. BSA-modified gold nanoclusters for sensing of folic acid. Sens Actuator, B Chem. 2014 Aug; 199:42–46. https://doi.org/10.1016/j.snb.2014.03.075

Housni A, Ahmed M, Liu S, Narain R. Monodisperse protein stabilized gold nanoparticles via a simple photochemical process. J Phys Chem C. 2008 Jul; 112(32):12282–12290. https://doi.org/10.1021/jp803890a

Huang X, Lan T, Zhang B, Ren J. Gold nanoparticle-enzyme conjugates-based FRET for highly sensitive determination of hydrogen peroxide, glucose and uric acid using tyramide reaction. Analyst. 2012 May; 137(16):3659–3666. https://doi.org/10.1039/C2AN35503E

Jastrebova J, Witthöft C, Grahn A, Svensson U, Jägerstad M. HPLC determination of folates in raw and processed beetroots. Food Chem. 2003 Apr; 80(4):579–588. https://doi.org/10.1016/S0308-8146(02)00506-X

Jiang DE, Tiago ML, Luo W, Dai S. The "staple" motif: A key to stability of thiolate-protected gold nanoclusters. J Am Chem Soc. 2008 Feb; 130(9):2777–2779. https://doi.org/10.1021/ja710991n

Kelly KL, Coronado E, Zhao LL, Schatz GC. The optical properties of metal nanoparticles: The influence of size, shape, and dielectric environment. J Phys Chem B. 2003 Dec; 107(3):668–677. https://doi.org/10.1021/jp026731y

Laemmli UK. Cleavage of structural proteins during the assembly of the head of bacteriophage T4. Nature. 1970 May; 227:680–685. https://doi.org/10.1038/227680a0

Lee YF, Huang CC. Colorimetric assay of lead ions in biological samples using a nanogold-based membrane. ACS Appl Mater Interfaces. 2011 June; 3(7):2747–2754. https://doi.org/10.1021/am200535s

Liang L, Subirade M. β-lactoglobulin/folic acid complexes: Formation, characterization, and biological implication. J Phys Chem B. 2010 Apr; 114(19):6707–6712. https://doi.org/10.1021/jp101096r

Lookhart G, Bean S. Separation and characterization of wheat protein fractions by high-performance capillary electrophoresis. Cereal Chem. 1995; 72(6):527-532. Available from: https://www.cerealsgrains.org/publications/cc/backissues/1995/Documents/72_527.pdf

Matei I, Buta CM, Turcu IM, Culita D, Munteanu C, Ionita G. Formation and stabilization of gold nanoparticles in bovine serum albumin solution. Molecules. 2019 Sept; 24(18):3395. https://doi.org/10.3390/molecules24183395

Mathew MS, Joseph K. Green synthesis of gluten-stabilized fluorescent gold quantum clusters: application as turn-on sensing of human blood creatinine. ACS Sustain Chem Eng. 2017 May; 5(6):4837–4845. https://doi.org/10.1021/acssuschemeng.7b00273

Mote US, Patil SR, Bhosale SH, Han SH, Kolekar GB. Fluorescence resonance energy transfer from tryptophan to folic acid in micellar media and deionised water. J Photochem Photobiol B Biol. 2011 Apr; 103(1):16–21. https://doi.org/10.1016/j.jphotobiol.2011.01.006

Nagaraja P, Vasantha RA, Yathirajan HS. Spectrophotometric determination of folic acid in pharmaceutical preparations by coupling reactions with iminodibenzyl or 3-aminophenol or sodium molybdate-pyrocatechol. Anal Biochem. 2002 Aug; 307(2):316–321. https://doi.org/10.1016/S0003-2697(02)00038-6

Rahman T, Hassan Chowdhury MM, Islam MT, Akhtaruzzaman M. Microbiological assay of folic acid content in some selected bangladeshi food stuffs. Int J Biol. 2015 Jan; 7(2):35–43. https://doi.org/10.5539/ijb.v7n2p35

Rajendran G, Rajamuthuramalingam T, Michael Immanuel Jesse D, Kathiravan K. Synthesis and characterization of biocompatible acetaminophen stabilized gold nanoparticles. Mater Res Express. 2019 Jul; 6(9): 095043. https://doi.org/10.1088/2053-1591/ab2e4d

Rastogi L, Kora AJ, Arunachalam J. Highly stable, protein capped gold nanoparticles as effective drug delivery vehicles for amino-glycosidic antibiotics. Mater Sci Eng C. 2012 Aug; 32(6):1571–1577. https://doi.org/10.1016/j.msec.2012.04.044

Ribeiro MV de M, Melo I da S, Lopes F das C da C, Moita GC. Development and validation of a method for the determination of folic acid in different pharmaceutical formulations using derivative spectrophotometry. Brazilian J Pharm Sci. 2016 Dec; 52(4):741–750. https://doi.org/10.1590/S1984-82502016000400019

Sandiford CP, Tatham AS, Fido R, Welch JA, Jones MG, Tee RD, et al. Identification of the major water/salt insoluble wheat proteins involved in cereal hypersensitivity. Clin Exp Allergy. 1997 Apr; 27(10):1120–1129. https://doi.org/10.1111/j.1365-2222.1997.tb01148.x

Shi W, Wang Y, Zhang H, Liu Z, Fei Z. Probing deep into the binding mechanisms of folic acid with α-amylase, pepsin and trypsin: An experimental and computational study. Food Chem. 2017 Jul; 226:128–134. https://doi.org/10.1016/j.foodchem.2017.01.054

Singh J, Blundell M, Tanner G, Skerritt JH. Albumin and globulin proteins of wheat flour: Immunological and N-terminal sequence characterisation. J Cereal Sci. 2001 Jul; 34(1):85–103. https://doi.org/10.1006/jcrs.2001.0380

Tan YN, Lee JY, Wang DIC. Uncovering the design rules for peptide synthesis of metal nanoparticles. J Am Chem Soc. 2010 Mar; 132(16):5677–5686. https://doi.org/10.1021/ja907454f

Veraverbeke WS, Delcour JA. Wheat protein composition and properties of wheat glutenin in relation to breadmaking functionality. Crit Rev Food Sci Nutr. 2002 May; 42(3):179–208. https://doi.org/10.1080/10408690290825510

Xie J, Zheng Y, Ying JY. Protein-directed synthesis of highly fluorescent gold nanoclusters. J Am Chem Soc. 2009 Jan; 131(3):888–889. https://doi.org/10.1021/ja806804u

Zheng J, Nicovich PR, Dickson RM. Highly fluorescent noble-metal quantum dots. Annu Rev Phys Chem. 2007 Aug; 58:409–431. https://doi.org/10.1146%2Fannurev.physchem.58.032806.104546

Zheng J, Zhou C, Yu M, Liu J. Different sized luminescent gold nanoparticles. Nanoscale. 2012 June; 4(14):4073–4083. https://doi.org/10.1039/C2NR31192E

Zhou C, Sun C, Yu M, Qin Y, Wang J, Kim M, et al. Luminescent gold nanoparticles with mixed valence states generated from dissociation of polymeric Au(I) thiolates. J Phys Chem C. 2010 Apr; 114(17):7727–7732. https://doi.org/10.1021/jp9122584

Zu L, Liu L, Qin Y, Liu H, Yang H. Multifunctional BSA-Au nanostars for photoacoustic imaging and X-ray computed tomography. Nanomed Nanotechnol Biol Med. 2016 Oct; 12(7):1805–1813. https://doi.org/10.1016/j.nano.2016.05.003